nature ecology & evolution

Article

https://doi.org/10.1038/s41559-022-01892-y

Coupled abiotic-biotic cycling of nitrous oxide in tropical peatlands

Received: 7 January 2022

Accepted: 26 August 2022

Published online: 06 October 2022

Check for updates

Steffen Buessecker[1,16], Analissa F. Sarno[1], Mark C. Reynolds[1], Ramani Chavan[2], Jin Park[2], Marc Fontánez Ortiz[1], Ana G. Pérez-Castillo[3], Grober Panduro Pisco[4], José David Urquiza-Muñoz[5,6,7], Leonardo P. Reis[8], Jefferson Ferreira-Ferreira[8], Jair M. Furtunato Maia[9,10], Keith E. Holbert[11], C. Ryan Penton[12], Sharon J. Hall[1], Hasand Gandhi[13,14], Iola G. Boëchat[15], Björn Gücker[15], Nathaniel E. Ostrom[13,14] and Hinsby Cadillo-Quiroz[1,2] ✉

Atmospheric nitrous oxide (N_2O) is a potent greenhouse gas thought to be mainly derived from microbial metabolism as part of the denitrification pathway. Here we report that in unexplored peat soils of Central and South America, N_2O production can be driven by abiotic reactions (≤98%) highly competitive to their enzymatic counterparts. Extracted soil iron positively correlated with in situ abiotic N_2O production determined by isotopic tracers. Moreover, we found that microbial N_2O reduction accompanied abiotic production, essentially closing a coupled abiotic-biotic N_2O cycle. Anaerobic N_2O consumption occurred ubiquitously (pH 6.4–3.7), with proportions of diverse clade II N_2O reducers increasing with consumption rates. Our findings show that denitrification in tropical peat soils is not a purely biological process but rather a 'mosaic' of abiotic and biotic reduction reactions. We predict that hydrological and temperature fluctuations differentially affect abiotic and biotic drivers and further contribute to the high N_2O flux variation in the region.

Nitrous oxide (N_2O), a potent greenhouse gas, has continued to accumulate in the Earth's atmosphere[1,2], calling for a better mechanistic understanding of its sources and sinks. Tropical soils are a major source of N_2O. The largest contribution to global N_2O flux, that is, the net effect of production and consumption, along with the highest uncertainties, have been observed over South America (~22.5%)[3–5] with large flux variations (−0.8 to 2,400 μg m^{-2} d^{-1}) described in ground-based measurements from extensive peatlands of the Amazon basin[6,7].

In waterlogged tropical peat soils, anoxic, reducing, humic acid-rich and Fe-holding conditions are favourable for the abiotic formation of N_2O[8]. Nitrous oxide can abiotically form from the reduction of nitrite (NO_2^-) via intermediary nitric oxide (NO) or hydroxylamine (NH_2OH)[9], both of which have typically low concentrations in soils.

[1]School of Life Sciences, Arizona State University, Tempe, AZ, USA. [2]Biodesign Institute, Arizona State University, Tempe, AZ, USA. [3]Environmental Pollution Research Center (CICA), University of Costa Rica, Montes de Oca, Costa Rica. [4]School of Forestry and Environmental Sciences, Ucayali National University, Ucayali, Peru. [5]Laboratory of Soil Research, Research Institute of Amazonia's Natural Resources, National University of the Peruvian Amazon, Iquitos, Loreto, Peru. [6]School of Forestry, National University of the Peruvian Amazon, Iquitos, Loreto, Peru. [7]Department for Biogeochemical Processes, Max Planck Institute for Biogeochemistry, Jena, Germany. [8]Mamiraua Institute for Sustainable Development, Amazonia, Brazil. [9]Normal Superior School, Amazonas State University, Manaus, Amazonia, Brazil. [10]National Institute of Amazonian Research, Manaus, Amazonia, Brazil. [11]School of Electrical, Computer and Energy Engineering, Arizona State University, Tempe, AZ, USA. [12]College of Integrative Sciences and Arts, Arizona State University, Mesa, AZ, USA. [13]Department of Integrative Biology, Michigan State University, East Lansing, MI, USA. [14]DOE Great Lakes Bioenergy Research Center, Michigan State University, East Lansing, MI, USA. [15]Applied Limnology Laboratory, Department of Geosciences, Federal University of São João del-Rei, São João del-Rei, Brazil. [16]Present address: Department of Earth System Science, Stanford University, Stanford, CA, USA. ✉e-mail: hinsby@asu.edu

Hydroxylamine conversion into N_2O relies on oxidants such as manganese (IV) minerals that are unlikely to persist in sufficient levels in the reducing milieu of peat. Thus, peatlands would generally favour the spontaneous chemical reduction of nitrogenous compounds—also called chemodenitrification. Some environments appear to sustain abiotic N_2O production rates based on dissolved Fe and Fe mineral phases[10–12], while others have shown an influence from organic matter (OM)[8], presumably by providing complexed Fe^{2+} and/or humic electron shuttles[13]. Abiotic N_2O formation has been recorded in polar[14] and temperate[14] environments, but the extent and distribution of this process in tropical peatlands have remained unexplored. With a recently estimated area of 1.7 million km^2 (ref. [14]), tropical peatlands under varying climatic regimes could play a major role in global N_2O gas cycling.

Denitrification, generally occurring at oxygen concentrations below 6 μM[14], is considered to be driven predominantly by microbial communities using Fe- and Cu-dependent reductase enzymes[14] through a modular pathway structure, with different populations mediating only one or two reduction steps[15]. Denitrifying microbes are well adapted to the conditions found in peat soils because they anaerobically respire organic substrates using nitrogen oxides as terminal electron acceptors[16]. Also, the extensive N_2O sink potential previously observed in diverse soils[17,18] can be better explained with the discovery of the abundant clade II N_2O-reducing bacteria. While clade I N_2O reducers are affiliated to the *Proteobacteria*, clade II N_2O reducers are more diverse and scattered across multiple phyla[19]. Interestingly, the clade II members tend to lack NO_2^- reductases more so than clade I members[19]. From an ecological perspective, this trait might correspond with an intrinsic capability of the soil habitat to reduce NO_2^- via chemodenitrification. Cellular resources can be saved and relocated to the expression of NO and N_2O reductases[20] to catalyse a thermodynamically more favourable redox reaction (ΔG of N_2O reduction is ~100 kJ mol^{-1} higher than ΔG of NO_2^- reduction).

While interactions between microbial guilds have been proposed as the basis for modularity[18], the interplay of denitrifiers with abiotic reactions has received little attention, even though chemodenitrification can reduce or contribute to different inorganic nitrogen pools, including N_2O and NO. The compatibility of abiotic N_2O production and modular microbial denitrification led us to hypothesize that a coupled abiotic-biotic N_2O cycle could operate in tropical peatlands. To test our hypothesis, we explored the dynamics and underlying factors of abiotic N_2O formation and microbial N_2O reduction in six geochemically diverse peatlands located across Central and South America at different altitudes using isotopic tracers. Simultaneously, we quantified and sequenced the *nosZ* gene as a marker for the N_2O-reducing microbial community. Our results provide evidence for concomitant abiotic N_2O production and microbial consumption active under various peat soil conditions.

Results

Fe^{2+} drives abiotic formation of N_2O in high-N_2O soils

We assessed soil denitrification in six pristine and managed tropical peatlands, four of which are located within or near the Amazon basin (San Jorge, SJO; Melendez, MEL; Sítio do Cacau, SCB; Fazenda Córrego da Areia, FCA) and two in Central America (Medio Queso, MQE; Las Vueltas, VUL; see Methods for further site description). The peatland altitudes sometimes differed by >2,000 m and were followed by a soil temperature span of over 16 °C (Fig. 1). Measured steady-state concentrations of NO_2^- in soil pore water were below detection (<1 μM) in the majority of sites, indicating rapid cycling[21,22]. The iron content and redox balance were highly variable, with higher Fe^{2+} concentrations in mountainous peat (~5 mM) and lower Fe^{2+} in oligotrophic peat (0.01–0.04 mM). To determine abiotic N_2O production rates under near-natural conditions, we induced a 10-fold spike with $^{15}NO_2^-$ in situ and measured $^{14}N^{15}NO + {}^{15}N^{14}NO + {}^{15}N^{15}NO$ evolution. Biotic activity was arrested by amending the soil with 87.5 mM $ZnCl_2$. Because the addition of Zn can liberate Fe^{2+} ions inevitably stimulating N_2O production[8], we repeated the soil incubations in the laboratory with 100 μM NO_2^- using both gamma-irradiated and Zn-treated peat soil. We then deduced a site-specific correction factor for estimates of in situ rates (Supplementary Information). All our reported abiotic N_2O production rates are therefore corrected for Zn-induced N_2O production.

Abiotic N_2O production was observed in all peatlands. On the basis of anoxic microcosms incubated on site, N_2O production rates ranged from low (0.05–0.3 nmol N_2O g^{-1} d^{-1}) at FCA and SCB, moderate (2.4–3.3 nmol N_2O g^{-1} d^{-1}) at MQE and SJO, and high (9.2–39.0 nmol N_2O g^{-1} d^{-1}) at MEL and VUL. Abiotic N_2O production contributed to the overall production to a greater extent than biotic N_2O production at half of the field sites (Fig. 1). Soil Fe^{2+} concentrations measured after extraction positively correlated with abiotic N_2O production rates ($R^2 > 0.99$, $n = 6$, Supplementary Fig. 1). To determine the nitrogen yield of the chemodenitrification reaction, we incubated gamma-irradiated and non-irradiated peat soil under anoxic conditions with 100 μM NO_2^-, and quantified NO_2^-, NO and N_2O in time (Supplementary Fig. 2). In two peatlands (SJO, SCB), complete nitrogen conversion into the gaseous phase was achieved based on almost purely abiotic reactions (Table 1). The reduction of NO_2^- resulted in varying NO and N_2O yields across sites, suggesting unequal nitrogen diversion directed by local peat chemistry. Our analytical approach could not confirm N_2 as a byproduct[23], which was presumably dominant at circum-neutral pH sites (MEL and VUL). We used this observed divergent NO_2^- conversion to group the diverse peat soils into high-N_2O (MQE, VUL, MEL) and high-NO (FCA, SJO, SCB) abiotic-yield sites (Table 1).

To our knowledge, this study represents a unique assessment of the relative contribution of abiotic N_2O production to the overall N_2O production at near-natural NO_2^- levels. Based on our results, abiotic reactions outcompete biotic reactions in three peatlands and are highly competitive as a source of N_2O at another two. The measured N_2O production rates were comparable to reported rates from a coniferous forest and grasslands[24], although the amount of added NO_2^- was at least one order of magnitude lower in our study. Relative to other evaluated ecosystems[10], peat soils have less oxidized Fe or Mn minerals and are enriched in recalcitrant organic carbon, which would hold additional reducing power, particularly in the structurally disparate OM. For instance, pi-electron bonds are an integral part of the chemical structures found in recalcitrant organic carbon, such as phenolic or humic substances, and they are prone to interact with NO_2^- (refs. [25,26]). Besides serving as reactants, humic substances can act as regenerable electron shuttles for redox reactions in soils and sediments[27]. Iron reduction and dissolution are greatly enhanced in the presence of humic substances[28,29], which increases the availability of Fe^{2+}. The distinct production of NO and N_2O across a gradient of Fe^{2+} concentrations suggests divergent reaction mechanisms in high-NO and high-N_2O soils. Previous reports agree with our data that indicate the larger production of NO as the final product of chemodenitrification, which is stimulated by the self-decomposition of nitrous acid in increasingly acidic soil milieu[30,31]. High-N_2O soils coincided with high soil Fe^{2+} abundances, and high-NO sites were associated with low Fe^{2+} (Fig. 1 and Table 1). Besides Fe^{2+}, the mixture of functional groups in peat OM may also be crucial in determining the NO to N_2O balance. Except for dimethyl glyoxime and quinone oximes, oxime groups preferentially produce N_2O and aromatics tend to produce NO[32].

Active microbial N_2O reduction in acidic peat soils

Concomitant with N_2O production, we measured N_2O consumption in anoxic microcosms incubated on site. Only non-sterilized samples exhibited active consumption. In sterilized samples, N_2O was a stable end-product after NO_2^- addition, and $^{15}N_2$ was not produced in $(^{15}N)_2O$ amendments. Incubations with $(^{15}N)_2O$ in the field resulted in an accumulation of the ^{15}N label in N_2 (Fig. 2) and were used to derive N_2O reduction rates. Enrichment of $^{15}N_2$ decreased

https://doi.org/10.1038/s41559-022-01892-y

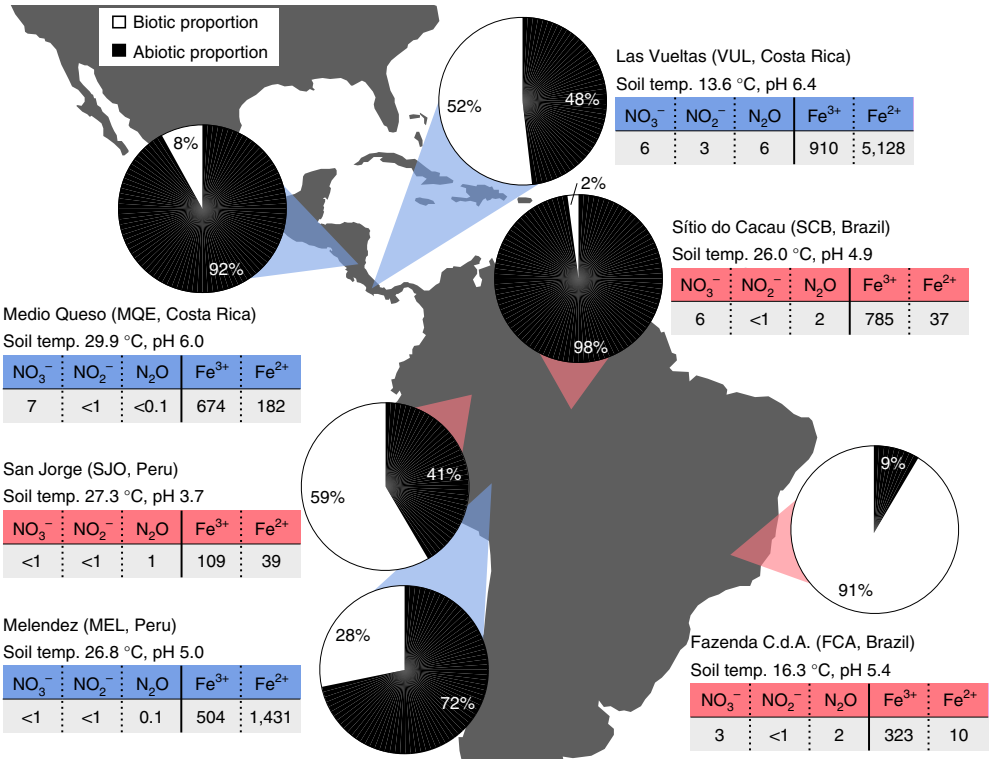

Fig. 1 | Contribution of abiotic and biotic reactions to overall N_2O production in tropical peatlands. Rates were derived in situ from the enrichment of ^{15}N in N_2O after addition of $^{15}NO_2^-$ to soil in the field ($n = 4$). Dissolved nitrogen (measured in situ) and Fe species (extracted) concentrations are given in µM. Sites are colour-coded on the basis of their NO to N_2O yield (Table 1), showing high-NO yield (red shades) or high-N_2O yield (blue shades).

Table 1 | Abiotic nitrogen yield fractions based on sterilized batch incubations

	SCB	SJO	FCA	MEL	VUL	MQE
Yield in NO (%)	97.2±12.7	92.8±17.4	74.3±20.8	0.2±0.03	0.2±0.01	1.3±0.3
Yield in N_2O (%)	4.8±0.2	4.8±0.4	4.0±0.6	12.1±0.5	24.6±1.8	55.9±2.8
Total yield (%)	102	97.6	78.3	12.3	24.8	57.2

Gamma-irradiated peat soil was used for anoxic incubations initiated with the addition of 100 µM NO_2^-. Yield was calculated using the molar fraction [NO-N or N_2O-N]/[NO_2^--N] after all NO_2^- was consumed and on the basis of stable NO and N_2O concentrations in at least two consecutive measurements. Sites with replicated samples (mean±95% CI, $n = 4$) are abbreviated as in Fig. 1.

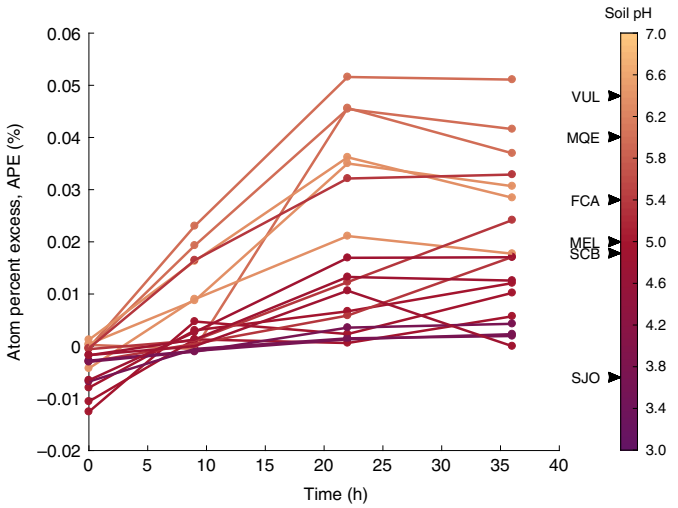

Fig. 2 | Isotopic enrichment in molecular nitrogen during in situ incubations of $(^{15}N)_2O$ with anoxic peat soil. Replicates per site ($n = 3$), as listed, are coloured in a gradient according to their pH. Site names abbreviated as in Fig. 1.

with soil pH (Fig. 2), while N_2O reduction was surprisingly observed in soils with pH as low as 3.7 (SJO). This finding is remarkable because N_2O reductase assembly is post-transcriptionally inhibited by acidic pH[33], and exposure to pH <4 disrupts a histidine amino acid ligand to the Cu cofactor in N_2O reductase, possibly inactivating the catalytic function (personal communication, W. Nitschke). The measured N_2O reduction rates were higher than previously observed rates at similar acidic pH values[34] and would extend the known physiological limits for microbial N_2O consumption. Thus, these results demonstrate the presence and activity of N_2O-reducing communities adapted to a wide range of peat soil pH.

Diverse clade II N_2O reducers are associated with higher N_2O sink potential

To evaluate the relationship between the abiotic formation and microbial consumption of N_2O, we compared reaction rates against *nosZ* gene abundances. Both processes revealed similar trends ranging from low (0.1–0.3 nmol N_2O g^{-1} d^{-1}) in SCB and FCA to moderate (0.7–1.5 nmol N_2O g^{-1} d^{-1}) in MQE and SJO to high (3–9.5 nmol N_2O g^{-1} d^{-1}) in

https://doi.org/10.1038/s41559-022-01892-y

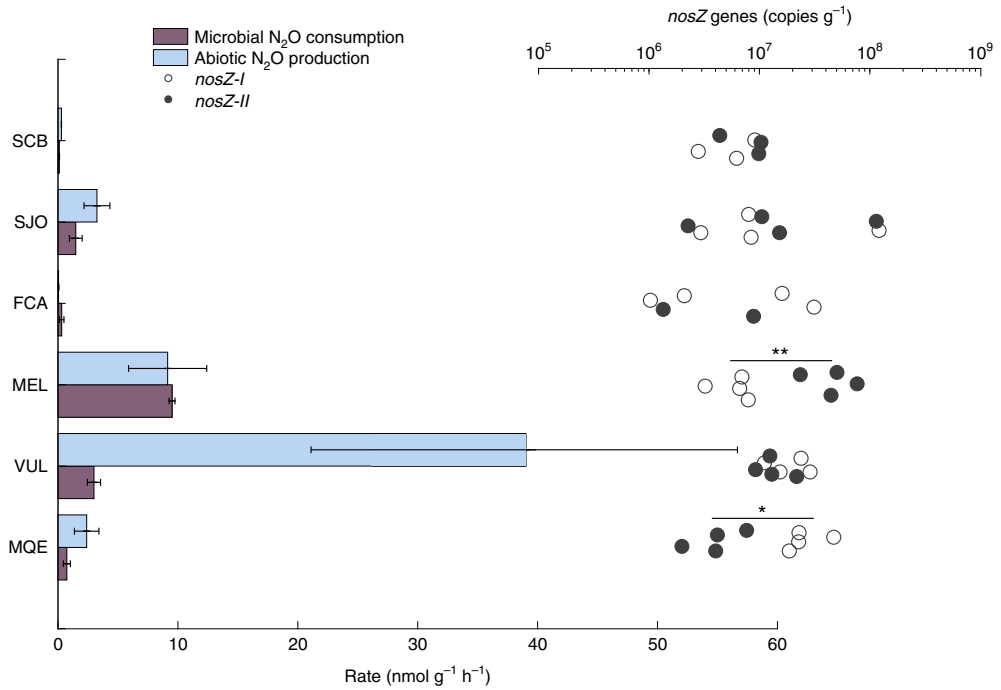

Fig. 3 | Microbial N_2O consumption and abiotic N_2O production (bars) along with *nosZ* gene quantities (open and filled circles). Error bars denote s.d. (consumption rates, $n = 3$; production rates, $n = 4$). Clade I and II *nosZ* were quantified by quantitative polymerase chain reactions (qPCR) assays and are significantly different within sites (ANOVA, $^*P = 0.012$, $^{**}P = 0.008$, $n = 4$). Two outliers for *nosZ-II* (SCB, ~6,200 copies g^{-1}; FCA, ~590) are not shown and another two datapoints are missing due to non-amplification. Site abbreviations as in Fig. 1.

VUL and MEL. Consumption never significantly exceeded production (Fig. 3). While the variation in *nosZ* gene copies from both clades showed no significant differences among high-NO sites (FCA, SJO, SCB), they differed (ANOVA, $P = 0.05$) among high-N_2O sites (MQE, MEL). Consumption rates gradually increased with clade II *nosZ* gene abundance at high-N_2O sites (Pearson's $r > 0.99$). A clear dominance of clade II *nosZ* genes over clade I coincided with the elevated rates of N_2O consumption in MEL peatland. Thus, N_2O reducers from clade II establish an increased microbial N_2O sink in peatlands with high abiotic N_2O production.

Next, to evaluate the N_2O-reducing microbial community, we analysed 183,265 and 80,050 taxonomically assigned *nosZ* gene amplicon sequence variants (ASVs) for clade I and II, respectively. Our analysis focused on the most abundant taxa that made up at least 1% of the total ASVs in at least one site (Fig. 4). The most abundant ASV was affiliated to the alpha-proteobacterium *Nitrospirillum amazonense* (Fig. 4). This phylotype constituted 59–64% of clade I ASVs in the Amazon bogs SCB and SJO but was least represented in the MEL peatland (~10%). In MEL, 23% of ASVs belonged to *Methylocystis* species, which were also abundant in FCA (27%). The clade II N_2O reducers were more diverse (comprised more phyla) across all soils (Fig. 4), with *Magnetospirillum* (consistently >10% in high-NO sites and 30% in VUL) and unclassified *Myxococcales* (8–50%) as the most abundant phylotypes. To examine the observed trend of N_2O reduction rates corresponding with *nosZ* clade II gene frequencies in the high-N_2O sites (MEL > VUL > MQE, Fig. 3), we derived diversity indices and performed a principal component analysis (PCA). The Shannon diversity index showed a coinciding order of diversity levels (1.73 > 1.49 > 1.39, Supplementary Tables 1a,b) for high-N_2O sites. This was also supported by a relatively high average Bray-Curtis dissimilarity of clade II *nosZ* gene sequences in MEL (0.71, Supplementary Tables 1c,d), identifying the clade II N_2O reducer community in this peatland as most dissimilar to all others. In addition, the community structure variation among clade II N_2O reducers was most parsimoniously explained by N_2O consumption rates in the PCA (Supplementary Figs. 3 and 4). Rather than being due to a single dominant taxon, a diverse group of clade II N_2O reducers appeared to be responsible for the high N_2O sink potential observed, consistent with studies on clade II distribution in temperate climates[35,36].

The intrinsic capacity of the peat to reduce NO_2^- abiotically could provide non-denitrifying microbes that do not possess denitrification enzymes other than N_2O reductase (called chemodenitrifiers[37]) an advantage over canonical denitrifiers. Chemodenitrifiers do not have to compete with chemodenitrification and simply harvest the end product N_2O to oxidize organic substrates. Figure 4 illustrates the NO_2^- reductase (either NirS or NirK) and NO reductase (NorB) enzyme repertoires present in available reference proteomes of relatives of the predicted taxa in both clades. At least 2 out of the 11 clade I taxa (including the abundant *Nitrospirillum*) and 10 out of the 14 clade II taxa indicated the absence of Nir enzymes (Fig. 4). Half of the clade II reference proteomes were missing both Nir and Nor proteins. Importantly, the Myxococcales ASVs showed no differences in abundance among high-NO sites but gradually increased, similar to the N_2O yield, in the high-N_2O sites. This order, which also includes *Anaeromyxobacter dehalogenans*—the hallmark organism of clade II N_2O reducers[17,38], is frequently represented in acidic, organic-rich soils[37,39], presumably with abiotic NO and N_2O production potential. Further, other bacteria such as *Dechloromonas*[40], *Ardenticatena*[41] and *Melioribacter*[42] also mediate iron reduction, an additional trait that could promote chemodenitrification by recycling Fe^{2+}. Therefore, chemodenitrifiers may outcompete canonical denitrifiers in the studied peatlands (for example, *Nitrospirillum*) due to higher affinity under low levels of substrate[43], and abundance patterns of the Myxococcales suggest a notable benefit for some chemodenitrifiers in soils associated with high abiotic N_2O yields.

Another abundant taxon of the N_2O-reducing community was *Magnetospirillum* (clade II) that includes several iron-oxidizing species. These alpha-proteobacteria synthesize the mixed-valence iron mineral magnetite, which can accumulate in soils, also under the influence of abiotic crystallization[44]. Secondary iron mineral formation can be

https://doi.org/10.1038/s41559-022-01892-y

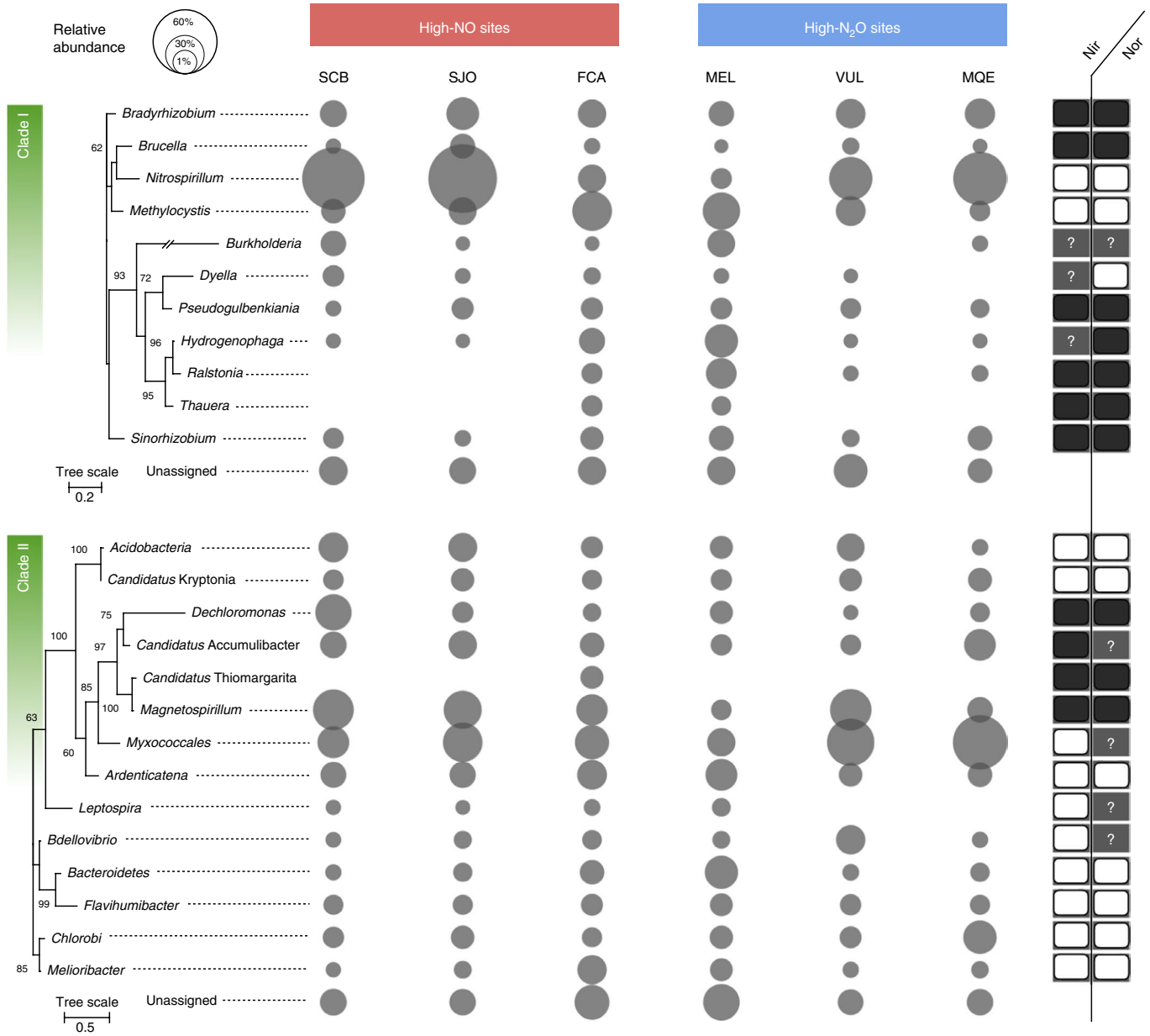

Fig. 4 | NosZ phylogeny and taxonomy in tropical peat soils. Only the most abundant ASVs >1% were included in the analysis. Maximum-likelihood phylogenetic trees are based on 1,000 iterations. Nodes with 60% or higher bootstrap support are labelled. The right panel indicates the presence (filled box) or absence (open box) of Nir or Nor enzyme sequences in reference proteomes. Boxes with question marks indicate an ambiguous distribution of Nir or Nor within the taxonomic group (Supplementary Table 2).

widespread in the tropics, driven by dissolved and particulate iron originating from weathering and desilication[45–47]. Ferrous iron-bearing minerals, such as magnetite, can serve as catalysts for NO_2^- reduction by providing reaction sites at the mineral surface[48,49]. The possession of an N_2O reductase makes sense for *Magnetospirillum*, assuming cells are associated with, or at least grow in proximity to, magnetite. Analyses of the iron phases present would be necessary to follow up on this in more detail, as this was outside the scope of our study. We also acknowledge that our insight into the temporal activity response is limited. Information on the actual in situ transcription levels is needed to better assess how the clades react to fluctuating abiotic pulses of N_2O[50].

Discussion

Our data show the co-occurrence of both abiotic N_2O production and microbial consumption (Fig. 3 and Supplementary Fig. 2), and their positive correlation points to the coupling of both processes in several sites (Supplementary Fig. 5). However, the mountain bog site (VUL) exhibited unusually high abiotic production rates and relatively low consumption rates (Fig. 3). A lower soil temperature than in the other peatlands and the differential sensitivity of production and consumption (Supplementary Table 3 and Supplementary Text) could lead to such kinetic effects[51–53]. Along these lines, the decoupling of production and consumption establishes the potential for vast N_2O emissions when changing environmental conditions impart selectively negative effects on consumption. For instance, while peatland drainage occurs naturally between wet and dry seasons[54], N_2O cycling could become decoupled by aerobic conditions created by extended peatland drainage, with microbial denitrification persisting only in anoxic microsites. Nitrite, fuelled by increased nitrification, could still be abiotically reduced to N_2O because acidic peat soil stabilizes Fe^{2+} via two mechanisms. First,

https://doi.org/10.1038/s41559-022-01892-y

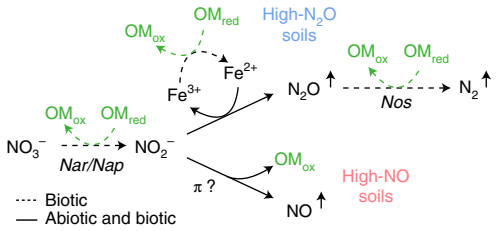

Fig. 5 | Schematic representation of denitrification pathways in tropical peatlands. NO_3^- reduction to NO_2^- occurs at substantial rates only with catalysis by NO_3^- reductases (Nar/Nap). Nitrite is rapidly reduced via abiotic and biotic reactions. At lower pH (≤5.4), NO is the dominant product. Nitrosation into OM may be an alternative abiotic process in soils with minor nitrogenous gas production reliant on organic compounds containing pi-electron bonds (π). In Fe^{2+}-rich peat, N_2O is the dominant product, involving Fe redox cycling that can fuel dissimilatory Fe reduction[11]. The only N_2O consumption pathway in peat soil is N_2O reductase-dependent reduction to N_2, which is active even in the most acidic soils tested (pH 3.7). All related heterotrophic reactions induce oxidation of OM ($OM_{red} \rightarrow OM_{ox}$) and eventually peat carbon mineralization.

Fe^{2+} oxidation by oxygen is kinetically hindered at low pH. Oxidation rates are considerably slowed at pH ≤6.5[55], a pH regime applying to most peatlands, including all in our study. Second, Fe^{2+} complexed by OM is resilient to oxidation. Experimental evidence suggests that tannic acid[56], phenolics[57], or natural humic acid[58] stabilize the Fe^{2+} pool in the presence of oxygen by the formation of a redox-buffering shell[58] and re-reduction of Fe^{3+}. However, little is known concerning how Fe^{2+} complexation affects NO_2^- accessibility and reduction. Nevertheless, these previous findings indicate that the reactants for chemodenitrification are sufficiently available even at higher oxygen concentrations (>6 µM), leading to a potential predominance of abiotic N_2O production over biotic N_2O production in peat soils.

We present evidence that active abiotic-biotic N_2O cycling is prevalent in tropical peatlands, where denitrification is not a purely biological pathway, but rather a 'mosaic' of biotic and abiotic reduction reactions (Fig. 5). Furthermore, our results support the idea that functional modularity complements not only the interrelationship of microbial groups but also concomitant interactions between microbes and spontaneous chemical reactions. Abiotic N_2O formation in tropical peatlands can have important regional consequences in the context of observed N_2O fluxes and higher rates in response to drainage[59] and putatively drought[60], as well as possible effects on reducing organic carbon release[61]. For example, compared with the other soils, abiotic N_2O production was moderate in SJO, an acidic oligotrophic site with a representative soil temperature of 27.3 °C, showing a net production of 1.8 nmol N_2O g^{-1} d^{-1}. With the estimation of the global extent of acidic oligotrophic tropical peatlands similar to SJO at 1,003,719 km^2 (ref. [62]), this could amount to a total depth-integrated abiotic N_2O flux ranging from 0.1 to 4.3 Tg N_2O yr^{-1} depending on the depth of NO_2^- diffusion. Given a factor of 298 g CO_2-equivalents per g N_2O over a 100 yr period[63], abiotic N_2O fluxes could alter the net radiative effect of tropical peatlands. Bypassing heterotrophic respiration through chemodenitrification, less organic carbon is mineralized to CO_2. Considering 4 moles of N_2O required to mineralize 1 mole of organic carbon, chemodenitrification could promote the retention of 0.3 Tg C yr^{-1} across oligotrophic tropical peatlands (Supplementary Text). These estimates are conservative because they do not include the diversion of nitrogen oxides into NO, nitrosation of OM and the consumption deficit observed in the high-altitude peatland. Sensitivity to lower temperatures could also impede microbial N_2O reduction in northern peatlands, which would imply an imbalanced cycling of N_2O and substantial N_2O release from abiotic origins.

Methods

Study sites

Six peatlands were chosen to cover a geochemical spectrum, including acidic (pH 3.7–5) soils, low (10 µM) and high (>5 mM) Fe^{2+} concentrations, varying OM content and soil temperature (Supplementary Table 4). Most sites were under little to no anthropogenic influence (Supplementary Table 5), with two exceptions: Fazenda Córrego da Areia (FCA) located within a catchment experiencing agricultural run-off in Brazil, and Medio Queso (MQE) in a Costa Rican river delta surrounded by agricultural run-off and cattle raising. The San Jorge (SJO) peatland is located in the Pastaza-Marañón foreland basin and Melendez (MEL) is in the Madre de Dios river terraces, both in Peru. Sítio do Cacau (SCB) is located in Central Amazonia (Amanã Reserve) in Brazil. Las Vueltas (VUL), located in Costa Rica's cloud forests of the Cerro Las Vueltas Reserve, differed most drastically from the other sites due to its higher altitude (2,500 m above sea level). Field work was conducted in September 2017 (Peru) and between April (Costa Rica) and July (Brazil) in 2018.

^{15}N tracer experiment in the field

Colorimetric assays to determine ambient soil NO_2^- and nitrate (NO_3^-) concentrations were performed in the field using a YSI 9500 portable spectrophotometer (YSI) including reagent kits, according to the manufacturer's instructions. Dissolved N_2O was sampled by collecting pore water into a pre-evacuated vial and subsequent degassing by shaking for 5 min. Thereafter, headspace was transferred into a pre-evacuated vial and stored underwater before analysis with a gas chromatograph equipped with an electron-capture detector (GC-ECD). Soil temperature and pH were measured with a YSI A10 pH probe (Ecosense, YSI).

Anaerobic glove bags filled with argon (Ar) were used to provide anaerobic conditions in the field while distributing soil into glass incubation vials (160 ml). Topsoils (10 cm) were sampled with 30-ml-barrel customized plastic corers. Inside the glove bag, the centre 5 cm (~15 g) soil was diluted 1:5 (w/v) into vials with anoxic water directly extracted from the same horizon via a water line connected to the glove bag. Separate sample sets received $^{15}NO_2^-$ (label fraction 0.1, Cambridge Isotopes) at 10× the soil ambient NO_2^- concentration and doubly labelled $(^{15}N)_2O$ (label fraction 1.0, Cambridge Isotopes) at 5× the soil ambient N_2O concentration. Thus, the amount of ^{15}N tracer applied varied slightly between sites but reflected a similar order of magnitude. $^{15}NO_2^-$ incubations included non-sterilized and 87.5 mM zinc chloride-poisoned ($ZnCl_2$, Thermo Fisher) soils in replicates of four ($n = 4$). Microcosms were shaken for 5 min after substrate addition to ensure optimal mixing of the label. Soil slurries were incubated in insulating containers to avoid temperature fluctuations on site, and gas samples were taken for $(^{15}N)_2O$ analysis at the beginning of incubation and after 24 h ($n = 4$), and for $^{30}N_2$ analysis at four time points spread over 36 h ($n = 3$). Gas sampling was destructive (entire headspace used) for $(^{15}N)_2O$ analysis or by replacement with 5 ml Ar gas for $^{30}N_2$ analysis. The sample times for the $^{30}N_2$ analysis were adapted from a previous study[64]. We also prepared zinc-poisoned $(^{15}N)_2O$ incubations to test for abiotic N_2O consumption. The gas samples were stored underwater in borosilicate glass vials closed with thick butyl rubber stoppers[65] before analysis at Michigan State University. Isotopic compositions of N_2O and N_2 were measured using an Elementar Isoprime isotope ratio mass spectrometer (IR-MS) interfaced with an Elementar TraceGas chromatographic system. Rate calculations closely followed a previously developed and tested protocol[66]. Given the constraints of sterilant applications in the field, we repeated the zinc-amended incubations in the laboratory, complementarily to incubations with gamma-irradiated soils. The rates from both experiments were used to calculate a correction factor accounting for artefacts caused by the zinc addition[8]. The rates derived in the field were then multiplied by the correction factor (Supplementary Fig. 6 and Table 6). The Brazilian sites SCB and FCA have associated data from gamma-irradiated soil, but data from zinc-treated soil are missing

because of logistic issues concerning the shipment of non-sterilized (not gamma-irradiated) soil. The final rates were combined according to the following equation for net in situ N_2O formation:

$$B = M + C - A$$

where B is the biotic N_2O production rate, M is the mixed rate (from non-sterilized $^{15}NO_2^-$ incubations), C is the microbial N_2O consumption rate (from $(^{15}N)_2O$ incubations) and A is the abiotic N_2O production rate (from poisoned $^{15}NO_2^-$ incubations).

Laboratory incubations

In an anoxic glove box (0.1% H_2 for O_2 reduction in N_2), gamma-sterilized and zinc-treated soil were prepared separately. Gamma sterilization followed a previous method[8]. Zinc chloride was applied as described for field experiments. The efficacy of sterilization techniques used was previously verified[8] and absence of biological activity was confirmed by steady CO_2 concentrations. Roots and coarse particles (>5 mm in diameter) were removed from soils, and soils were slurried 1:5 (w/v) in anoxic, sterile 18.2 MΩ·cm water. The slurry was homogenized before equal quantities were distributed into culture vials and sealed with sterile butyl rubber stoppers. An anoxic and filter-sterilized NO_2^- solution was injected (final concentration 100 µM) into microcosms that were previously flushed with pure N_2. The microcosms were agitated briefly to disperse the added substrate and then kept under dark, static conditions at room temperature for ~100 h. Dissolved NO_2^- was quantified with the Griess reagent (Promega, kit G2930), and NO and N_2O were analysed as described below. Extended Data Fig. 1 illustrates the workflow of field and laboratory incubations.

Soil Fe measurements

Soils for Fe analysis were kept in anoxic serum bottles and refrigerated during transport. The species Fe^{2+} and Fe^{3+} were extracted and separated as previously described[8] and quantified in acidified aqueous solution by inductively coupled plasma–optical emission spectrometry (ICP-OES; Thermo iCAP6300 at the Goldwater Environmental Laboratory at Arizona State University). The ICP-OES pump rate for the Ar carrier was set to 50 r.p.m., and Fe2395 and Fe2599 lines were used for Fe quantification. Iron concentrations were determined from a calibration curve (0.01–10 mg l^{-1}) by diluting a standard solution (100 mg l^{-1}, VHG Labs, SM75B-500) in 0.02 N HNO_3.

N_2O gas measurements

Using a gas-tight syringe (VICI Precision Sampling), 200 µl of gas sample was injected into a GC-ECD (SRI Instruments). Two continuous HayeSep-D columns were kept at 90 °C (oven temperature), and N_2 (UHP grade 99.999%, Praxair) was used as carrier gas. The ECD current was 250 mV, and the ECD cell was kept at 350 °C. The N_2O measurements were calibrated over a range of 0.25–100 ppmv using customized standard mixtures (Scott Specialty Gases, accuracy ±5%). Gas concentrations were corrected for solubility effects using Henry's law and the dimensionless concentration constant $k_H^{cc}(N_2O) = 0.6112$ to account for gas partitioning into the aqueous phase at 25 °C and 1 atm[67].

NO gas measurements

NO was quantified in the microcosm headspace with a chemiluminescence-based analyser (LMA-3D NO_2 analyser, Unisearch). Headspace gas (50 µl) was withdrawn with a CO_2-N_2-flushed gas-tight syringe and injected into the analyser. The injection port was customized to fit the injection volume and consisted of a T-junction with an air filtre at one end and a septum at the other end. An internal pump generated consistent airflow. Our method followed a previous protocol[68], with minor adjustments. Briefly, NO was oxidized to NO_2 by a CrO_3 catalyst. The NO_2 was carried across a fabric wick saturated with a Luminol solution (Drummond Technology). Readings were corrected for background NO_2 every 15 min ('zeroing'). Shell airflow rate was kept at 500 ml min^{-1}, and the span potentiometer was set to 8. Measurements were calibrated with a 0.1 ppm NO (in N_2) standard (<0.0005 ppm NO_2, Scott-Marrin) over a range of 5–1,000 ppbv. Gas concentrations were corrected using Henry's law and the dimensionless concentration constant $k_H^{cc}(NO) = 0.0465$ to account for gas partitioning into the aqueous phase at 25 °C and 1 atm[67].

Molecular analyses

Peat samples from four randomly distributed locations (coinciding with incubation locations) within a peatland were collected and frozen at −20 °C for subsequent DNA extraction. Genomic DNA was extracted using a NucleoSpin soil DNA extraction kit (Macherey-Nagel).

For quantitative PCR, we used primer pairs designed by Henry et al.[69] and Jones et al.[70] for clade I and II, respectively, and a total reaction volume of 15 µl with 1.5 µl DNA template (35–50 ng genomic DNA). The clade I *nosZ* gene was amplified with PowerUp SYBR Green master mix (Applied Biosystems), to which 3 mM $MgCl_2$ was added. Forward and reverse primer concentrations were 1 µM, and previous cycler conditions were used[69]. The clade II *nosZ* gene was amplified using SYBR Fast, ROX low master mix (Kapa Biosystems, Roche) and 1.2 µM primer concentration[70]. Thermal cycling was initiated with 3 min of denaturation at 95 °C, followed by 40 cycles of the following stages: 30 s at 95 °C, 60 s at 58 °C, 30 s at 72 °C, 30 s at 80 °C, and a final melting curve. Samples were run in technical duplicates on 96-well plates using a Quantstudio 3 thermocycler (Applied Biosystems). Standards were prepared using linearized plasmids. Standard curves indicated efficiencies of 94% ($R^2 = 0.99$, *nosZ* clade I) and 85% ($R^2 = 0.99$, *nosZ* clade II), and melting curves showed no detectable primer dimers over the duration of 40 amplification cycles.

For Illumina amplicon sequence analysis, we developed independent *nosZ* clade I and II libraries. PCR amplification of both *nosZ* genes used the Promega GoTaq qPCR kit (Promega) and 1 µl of DNA template (25–50 ng genomic DNA) in a total reaction volume of 20 µl. Targeting the clade I *nosZ* gene, we used a novel primer pair[71]. The reaction mix included 0.2 mg ml^{-1} bovine serum albumin (BSA) and 0.8 µM primer concentration. For the clade II *nosZ* gene, we used the same primer as for qPCR in reactions of 1 mg ml^{-1} BSA and 0.8 µM primer concentration. Cycling conditions for clade II *nosZ* amplification were used as previously described[70]. Thermal cycling conditions for clade I *nosZ* amplification were an initial 2 min denaturation step at 95 °C, followed by 33 cycles of 95 °C for 45 s, annealing at 53 °C for 45 s, a 72 °C extension for 30 s, and a final extension at 72 °C for 7 min. Amplification was verified by gel electrophoresis using 1% agarose in 1 Tris-acetate-EDTA buffer. Samples were multiplexed[72], normalized (SequalPrep 1051001, Invitrogen), and submitted for sequencing to the DNASU core facility at Arizona State University, with 2× 300 bp paired-end Illumina MiSeq.

Paired-end sequences were merged and demultiplexed, then we used the USEARCH pipeline[73] to (1) correct strand orientations, (2) sort out singletons and (3) denoise the dataset. We used alpha = 2 for a stringent denoising of sequences[74] because reads were not clustered with any identity radius to obtain ASVs. The sequences were translated and frameshift-corrected by Framebot[75] with low sequence loss (<10%). The amino acid sequences obtained were classified using Diamond[76] version 0.9.25. The search was conducted in Diamond's 'sensitive' mode, with an *e*-value cut-off of 10^{-5}, resulting in the top 5% hits. Sequences were parsed through two databases: the NCBI database RefSeq (release 95) containing 146,381,777 non-redundant protein sequences and manually curated databases built from 2,817 (clade I) and 2,929 (clade II) sequences off the FunGene repository[77] using the search parameters 80% hidden Markov model (HMM) coverage and a minimum length of 550 amino acids. The taxonomy achieved with the curated databases was used for downstream analysis because of a higher number of classified sequences. The output was imported into Megan[78] version 6.18.0, where a weighted lowest common ancestor

algorithm (default parameters according to ref. [79].) was run to assign a single taxonomic lineage to each read. ASV tables were pasted into Krona[80] for visual inspection of results. Reads with abundances >1% in at least one site were extracted, and consensus sequences were determined for each taxonomic group. Maximum-likelihood phylogenetic trees were constructed with consensus sequences in Mega X[81]. To infer presence/absence of Nir and Nor enzymes in representative proteomes, UniProt reference (manually curated) proteomes were screened using BlastP with default parameters. NirS (Q51700, *Paracoccus denitrificans* PD1222), NirK (O31380, *Bradyrhizobium japonicum*), NorB (Q51663, *Paracoccus denitrificans*) were used as amino acid query sequences.

The *nosZ* sequences have been deposited in the GenBank, EMBL and DDBJ databases as SRA Bioproject PRJNA834844.

Statistical analyses

All statistical tests were performed with JMP Pro software (Version 13.1.0, SAS Institute). Analysis of variance (ANOVA) was used with $P < 0.05$ to test for significantly different values for gene quantities across soils. Plotting and regression analysis were done with the Matlab R2018a software package (Version 9.4.0.813654, Mathworks).

Reporting summary

Further information on research design is available in the Nature Research Reporting Summary linked to this article.

Data availability

All data to evaluate the conclusions of the study are present in the paper and its Supplementary Information and can be found in the Figshare repository (https://doi.org/10.6084/m9.figshare.19552588.v1). Genomic data have been deposited in the GenBank, EMBL, and DDBJ databases under accession: SAMN27959396, SAMN27959397, SAMN27959398, SAMN27959399, SAMN27959400, SAMN27959401, SAMN27959402, SAMN27959403, SAMN27959404, SAMN27959405, SAMN27959406, SAMN27959407, SAMN27959408, SAMN27959409, SAMN27959410, SAMN27959411, SAMN27959412, SAMN27959413, SAMN27959414, SAMN27959415, SAMN27959416, SAMN27959417, SAMN27959418, SAMN27959419, SAMN27959420, SAMN27959421, SAMN27959422, SAMN27959423, SAMN27959424, SAMN27959425, SAMN27959426, SAMN27959427, SAMN27959428, SAMN27959429, SAMN27959430, SAMN27959431, SAMN27959432, SAMN27959433, SAMN27959434, SAMN27959435, SAMN27959436, SAMN27959437, SAMN27959438, SAMN27959439, SAMN27959440, SAMN27959441, SAMN27959442 and SAMN27959443

References

1. Thompson, R. L. et al. Acceleration of global N_2O emissions seen from two decades of atmospheric inversion. *Nat. Clim. Change* **9**, 993–998 (2019).
2. Tian, H. et al. A comprehensive quantification of global nitrous oxide sources and sinks. *Nature* **586**, 248–256 (2020).
3. Zhuang, Q., Lu, Y. & Chen, M. An inventory of global N_2O emissions from the soils of natural terrestrial ecosystems. *Atm. Environ.* **47**, 66–75 (2012).
4. Huang, J. et al. Estimation of regional emissions of nitrous oxide from 1997 to 2005 using multinetwork measurements, a chemical transport model, and an inverse method. *J. Geophys. Res.* **113**, D17313 (2008).
5. D'Amelio, M. T. S., Gatti, L. V., Miller, J. B. & Tans, P. Regional N_2O fluxes in Amazonia derived from aircraft vertical profiles. *Atmos. Chem. Phys.* **9**, 8785–8797 (2009).
6. Teh, Y. A., Murphy, W. A., Berrio, J.-C., Boom, A. & Page, S. E. Seasonal variability in methane and nitrous oxide fluxes from tropical peatlands in the western Amazon basin. *Biogeosciences* **14**, 3669–3683 (2017).
7. Finn, D. R. et al. Methanogens and methanotrophs show nutrient-dependent community assemblage patterns across tropical peatlands of the Pastaza-Marañón Basin, Peruvian Amazonia. *Front. Microbiol.* **11**, 746 (2020).
8. Buessecker, S. et al. Effects of sterilization techniques on chemodenitrification and N_2O production in tropical peat soil microcosms. *Biogeosciences* **16**, 4601–4612 (2019).
9. Heil, J., Liu, S., Vereecken, H. & Brüggemann, N. Abiotic nitrous oxide production from hydroxylamine in soils and their dependence on soil properties. *Soil Biol. Biochem.* **84**, 107–115 (2015).
10. Samarkin, V. A. et al. Abiotic nitrous oxide emission from the hypersaline Don Juan Pond in Antarctica. *Nat. Geosci.* **3**, 341–344 (2010).
11. Otte, J. M. et al. N_2O formation by nitrite-induced (chemo) denitrification in coastal marine sediment. *Sci. Rep.* **9**, 10691 (2019).
12. Jones, L. C., Peters, B., Pacheco, J. S. L., Casciotti, K. L. & Fendorf, S. Stable isotopes and iron oxide mineral products as markers of chemodenitrification. *Environ. Sci. Technol.* **49**, 3444–3452 (2015).
13. Tolman, W. B. Binding and activation of N_2O at transition-metal centers: recent mechanistic insights. *Angew. Chem. Int. Ed.* **49**, 1018–1024 (2010).
14. Holtan-Hartwig, L., Dörsch, P. & Bakken, L. R. Low temperature control of soil denitrifying communities: kinetics of N_2O production and reduction. *Soil Biol. Biochem.* **34**, 1797–1806 (2002).
15. Gorelsky, S. I., Ghosh, S. & Solomon, E. I. Mechanism of N2O reduction by the μ4-S tetranuclear CuZ cluster of nitrous oxide reductase. *J. Am. Chem. Soc.* https://doi.org/10.1021/ja055856o (2005).
16. Tsai, M.-L. et al. $[Cu_2O]^{2+}$ active site formation in Cu–ZSM-5: geometric and electronic structure requirements for N_2O activation. *J. Am. Chem. Soc.* https://doi.org/10.1021/ja4113808 (2014).
17. Sanford, R. A. et al. Unexpected nondenitrifier nitrous oxide reductase gene diversity and abundance in soils. *Proc. Natl Acad. Sci. USA* **109**, 19709–19714 (2012).
18. Jones, C. M. et al. Recently identified microbial guild mediates soil N_2O sink capacity. *Nat. Clim. Change* **4**, 801–805 (2014).
19. Hallin, S., Philippot, L., Löffler, F. E., Sanford, R. A. & Jones, C. M. Genomics and ecology of novel N_2O-reducing microorganisms. *Trends Microbiol.* **26**, 43–55 (2018).
20. Lycus, P. et al. A bet-hedging strategy for denitrifying bacteria curtails their release of N2O. *Proc. Natl Acad. Sci. USA* **115**, 11820–11825 (2018).
21. Burns, L. C., Stevens, R. J. & Laughlin, R. J. Determination of the simultaneous production and consumption of soil nitrite using ^{15}N. *Soil Biol. Biochem.* **27**, 839–844 (1995).
22. Burns, L. C., Stevens, R. J. & Laughlin, R. J. Production of nitrite in soil by simultaneous nitrification and denitrification. *Soil Biol. Biochem.* **28**, 609–616 (1996).
23. Wullstein, L. H. & Gilmour, C. M. Non-enzymatic formation of nitrogen gas. *Nature* **210**, 1150–1151 (1966).
24. Liu, S., Schloter, M., Hu, R., Vereecken, H. & Brüggemann, N. Hydroxylamine contributes more to abiotic N2O production in soils than nitrite. *Front. Environ. Sci.* https://doi.org/10.3389/fenvs.2019.00047 (2019).
25. Thorn, K. A. & Mikita, M. A. Nitrite fixation by humic substances: nitrogen-15 nuclear magnetic resonance evidence for potential intermediates in chemodenitrification. *Soil Sci. Soc. Am. J.* **64**, 568–582 (2000).

26. Thorn, K. A., Younger, S. J. & Cox, L. G. Order of functionality loss during photodegradation of aquatic humic substances. *J. Environ. Qual.* **39**, 1416–1428 (2010).
27. Klüpfel, L., Piepenbrock, A., Kappler, A. & Sander, M. Humic substances as fully regenerable electron acceptors in recurrently anoxic environments. *Nat. Geosci.* **7**, 195–200 (2014).
28. Lovley, D. R. & Blunt-Harris, E. L. Role of humic-bound iron as an electron transfer agent in dissimilatory Fe(III) reduction. *Appl. Environ. Microbiol.* **65**, 4252–4254 (1999).
29. Kappler, A., Benz, M., Schink, B. & Brune, A. Electron shuttling via humic acids in microbial iron(III) reduction in a freshwater sediment. *FEMS Microbiol. Ecol.* **47**, 85–92 (2004).
30. Van Cleemput, O., Patrick, W. H. & McIlhenny, R. C. Nitrite decomposition in flooded soil under different pH and redox potential conditions. *Soil Sci. Soc. Am. J.* **40**, 55–60 (1976).
31. Van Cleemput, O. & Baert, L. Nitrite: a key compound in N loss processes under acid conditions? *Plant Soil* **76**, 233–241 (1984).
32. Porter, L. K. Gaseous products produced by anaerobic reaction of sodium nitrite with oxime compounds and oximes synthesized from organic matter. *Soil Sci. Soc. Am. J.* **33**, 696–702 (1969).
33. Liu, B., Mørkved, P. T., Frostegård, Å. & Bakken, L. R. Denitrification gene pools, transcription and kinetics of NO, N_2O and N_2 production as affected by soil pH. *FEMS Microbiol. Ecol.* **72**, 407–417 (2010).
34. Palmer, K., Biasi, C. & Horn, M. A. Contrasting denitrifier communities relate to contrasting N_2O emission patterns from acidic peat soils in arctic tundra. *ISME J.* **6**, 1058–1077 (2012).
35. Domeignoz-Horta, L. et al. The diversity of the N_2O reducers matters for the N2O:N2 denitrification end-product ratio across an annual and a perennial cropping system. *Front. Microbiol.* https://doi.org/10.3389/fmicb.2015.00971 (2015).
36. Domeignoz-Horta, L. A. et al. Peaks of in situ N_2O emissions are influenced by N_2O-producing and reducing microbial communities across arable soils. *Glob. Change Biol.* **24**, 360–370 (2018).
37. Onley, J. R., Ahsan, S., Sanford, R. A. & Löffler, F. E. Denitrification by *Anaeromyxobacter dehalogenans*, a common soil bacterium lacking the nitrite reductase genes *nirS* and *nirK*. *Appl. Environ. Microbiol.* **84**, 4 (2018).
38. Sanford, R. A., Cole, J. R. & Tiedje, J. M. Characterization and description of *Anaeromyxobacter dehalogenans* gen. nov., sp. nov., an aryl-halorespiring facultative anaerobic myxobacterium. *Appl. Environ. Microbiol.* **68**, 893–900 (2002).
39. Mohr, K. I., Zindler, T., Wink, J., Wilharm, E. & Stadler, M. Myxobacteria in high moor and fen: an astonishing diversity in a neglected extreme habitat. *MicrobiologyOpen* **6**, e00464 (2017).
40. Hori, T., Müller, A., Igarashi, Y., Conrad, R. & Friedrich, M. W. Identification of iron-reducing microorganisms in anoxic rice paddy soil by ^{13}C-acetate probing. *ISME J.* **4**, 267–278 (2010).
41. Kawaichi, S. et al. *Ardenticatena maritima* gen. nov., sp. nov., a ferric iron- and nitrate-reducing bacterium of the phylum 'Chloroflexi' isolated from an iron-rich coastal hydrothermal field, and description of *Ardenticatenia* classis nov. *Int. J. Sys. Evol. Microbiol.* **63**, 2992–3002 (2013).
42. Podosokorskaya, O. A. et al. Characterization of *Melioribacter roseus* gen. nov., sp. nov., a novel facultatively anaerobic thermophilic cellulolytic bacterium from the class *Ignavibacteria*, and a proposal of a novel bacterial phylum Ignavibacteriae. *Environ. Microbiol.* **15**, 1759–1771 (2013).
43. Yoon, S. et al. Nitrous oxide reduction kinetics distinguish bacteria harboring clade I nosz from those harboring clade II NosZ. *Appl. Environ. Microbiol.* **82**, 3793–3800 (2016).
44. Maher, B. A. & Taylor, R. M. Formation of ultrafine-grained magnetite in soils. *Nature* **336**, 368–370 (1988).
45. Sanchez, P. A. *Properties and Management of Soils in the Tropics* (Wiley, 1976).
46. White, A. F. et al. Chemical weathering in a tropical watershed, Luquillo Mountains, Puerto Rico: I. Long-term versus short-term weathering fluxes. *Geochim. Cosmochim. Acta* **62**, 209–226 (1998).
47. Hall, S. J., Liptzin, D., Buss, H. L., DeAngelis, K. & Silver, W. L. Drivers and patterns of iron redox cycling from surface to bedrock in a deep tropical forest soil: a new conceptual model. *Biogeochemistry* **130**, 177–190 (2016).
48. Buchwald, C., Grabb, K., Hansel, C. M. & Wankel, S. D. Constraining the role of iron in environmental nitrogen transformations: dual stable isotope systematics of abiotic NO_2^- reduction by Fe(II) and its production of N_2O. *Geochim. Cosmochim. Acta* **186**, 1–12 (2016).
49. Grabb, K. C., Buchwald, C., Hansel, C. M. & Wankel, S. D. A dual nitrite isotopic investigation of chemodenitrification by mineral-associated Fe(II) and its production of nitrous oxide. *Geochim. Cosmochim. Acta* **196**, 388–402 (2017).
50. Drewer, J. et al. Linking nitrous oxide and nitric oxide fluxes to microbial communities in tropical forest soils and oil palm plantations in Malaysia in laboratory incubations. *Front. For. Glob. Change* **3**, 4 (2020).
51. Yvon-Durocher, G., Jones, J. I., Trimmer, M., Woodward, G. & Montoya, J. M. Warming alters the metabolic balance of ecosystems. *Phil. Trans. R. Soc. B* **365**, 2117–2126 (2010).
52. Yvon-Durocher, G. et al. Reconciling the temperature dependence of respiration across timescales and ecosystem types. *Nature* **487**, 472–476 (2012).
53. Jauhiainen, J., Kerojoki, O., Silvennoinen, H., Limin, S. & Vasander, H. Heterotrophic respiration in drained tropical peat is greatly affected by temperature – a passive ecosystem cooling experiment. *Environ. Res. Lett.* **9**, 105013 (2014).
54. Wang, S., Zhuang, Q., Lähteenoja, O., Draper, F. C. & Cadillo-Quiroz, H. Potential shift from a carbon sink to a source in Amazonian peatlands under a changing climate. *Proc. Natl Acad. Sci. USA* **115**, 12407–12412 (2018).
55. Stumm, W. & Lee, G. F. Oxygenation of ferrous iron. *Ind. Eng. Chem.* **53**, 143–146 (1961).
56. Theis, T. L. & Singer, P. C. Complexation of iron(II) by organic matter and its effect on iron(II) oxygenation. *Environ. Sci. Technol.* **8**, 569–573 (1974).
57. Wan, X. et al. Complexation and reduction of iron by phenolic substances: implications for transport of dissolved Fe from peatlands to aquatic ecosystems and global iron cycling. *Chem. Geol.* **498**, 128–138 (2018).
58. Daugherty, E. E., Gilbert, B., Nico, P. S. & Borch, T. Complexation and redox buffering of iron(II) by dissolved organic matter. *Environ. Sci. Technol.* **51**, 11096–11104 (2017).
59. Prananto, J. A., Minasny, B., Comeau, L.-P., Rudiyanto, R. & Grace, P. Drainage increases CO_2 and N_2O emissions from tropical peat soils. *Glob. Change Biol.* **26**, 4583–4600 (2020).
60. Stirling, E., Fitzpatrick, R. W. & Mosley, L. Drought effects on wet soils in inland wetlands and peatlands. *Earth Sci. Rev.* **210**, 103387 (2020).
61. Hodgkins, S. B. et al. Tropical peatland carbon storage linked to global latitudinal trends in peat recalcitrance. *Nat. Commun.* **9**, 3640 (2018).
62. Gumbricht, T. et al. An expert system model for mapping tropical wetlands and peatlands reveals South America as the largest contributor. *Glob. Change Biol.* **23**, 3581–3599 (2017).
63. IPCC *Climate Change 2021: The Physical Science Basis* (eds Masson-Delmotte, V. et al.) (Cambridge Univ. Press, 2021).
64. Babbin, A. R., Bianchi, D., Jayakumar, A. & Ward, B. B. Rapid nitrous oxide cycling in the suboxic ocean. *Science* **348**, 1127–1129 (2015).

65. Hamilton, S. K. & Ostrom, N. E. Measurement of the stable isotope ratio of dissolved N_2 in ^{15}N tracer experiments. *Limnol. Oceanogr. Methods* **5**, 233–240 (2007).
66. Ostrom, N. E., Gandhi, H., Trubl, G. & Murray, A. E. Chemodenitrification in the cryoecosystem of Lake Vida, Victoria Valley, Antarctica. *Geobiology* **14**, 575–587 (2016).
67. Stumm, W. & Morgan, J. J. *Aquatic Chemistry* 3rd edn (John Wiley & Sons, 1996).
68. Homyak, P. M., Kamiyama, M., Sickman, J. O. & Schimel, J. P. Acidity and organic matter promote abiotic nitric oxide production in drying soils. *Glob. Change Biol.* **23**, 1735–1747 (2017).
69. Henry, S., Bru, D., Stres, B., Hallet, S. & Philippot, L. Quantitative detection of the *nosZ* gene, encoding nitrous oxide reductase, and comparison of the abundances of 16S rRNA, *narG*, *nirK*, and *nosZ* genes in soils. *Appl. Environ. Microbiol.* **72**, 5181–5189 (2006).
70. Jones, C. M., Graf, D. R., Bru, D., Philippot, L. & Hallin, S. The unaccounted yet abundant nitrous oxide-reducing microbial community: a potential nitrous oxide sink. *ISME J.* **7**, 417–426 (2013).
71. Zhang, B. et al. A new primer set for clade I *nosZ* that recovers genes from a broader range of taxa. *Biol. Fertil. Soils* **57**, 523–531 (2021).
72. Herbold, C. W. et al. A flexible and economical barcoding approach for highly multiplexed amplicon sequencing of diverse target genes. *Front. Microbiol.* **6**, 8966 (2015).
73. Edgar, R. C. Search and clustering orders of magnitude faster than BLAST. *Bioinformatics* **26**, 2460–2461 (2010).
74. Edgar, R. C. UNOISE2: improved error-correction for Illumina 16S and ITS amplicon sequencing. Preprint at https://www.biorxiv.org/content/early/2016/10/15/081257 (2016).
75. Wang, Q. et al. Ecological patterns of *nifH* genes in four terrestrial climatic zones explored with targeted metagenomics using Framebot, a new informatics tool. *mBio* **4**, e00592-13 (2013).
76. Buchfink, B., Xie, C. & Huson, D. H. Fast and sensitive protein alignment using DIAMOND. *Nat. Methods* **12**, 59–60 (2015).
77. Fish, J. A. et al. FunGene: the functional gene pipeline and repository. *Front. Microbiol.* **4**, 291 (2013).
78. Huson, D. H. et al. MEGAN Community Edition - interactive exploration and analysis of large-scale microbiome sequencing data. *PLoS Comput. Biol.* **12**, e1004957 (2016).
79. Huson, D. H. et al. MEGAN-LR: new algorithms allow accurate binning and easy interactive exploration of metagenomic long reads and contigs. *Biol. Direct* **13**, 6 (2018).
80. Ondov, B. D., Bergman, N. H. & Phillippy, A. M. Interactive metagenomic visualization in a Web browser. *BMC Bioinformatics* **12**, 385 (2011).
81. Kumar, S., Stecher, G., Li, M., Knyaz, C. & Tamura, K. MEGA X: molecular evolutionary genetics analysis across computing platforms. *Mol. Biol. Evol.* **35**, 1547–1549 (2018).

Acknowledgements

We acknowledge R. T. Espinoza, T. P. Gomez, D. Reyna, B. Crnobrna, O. Lähteenoja, K. Arbaiza, A. H. Carmona, P. Fonteboa, R. C. Chaves, J. R. Trucios, C. M. Cadillo-Quiroz, the UFSJ Graduate Program in Geography (PPGEOG) and the Office for International Affairs (ASSIN/UFSJ) for assistance and help during stages of field work. We also thank W. Nitschke (CNRS/BIP) for discussions, M. Abdalla for efforts supporting this effort at the USAID-GDR program at ASU, and the USAID missions in Peru and Brazil.
This study was funded by an NSF-DEB award (no. 1355066) and a SOLS -KED ASU award (ECR A548 HC) to H.C-Q, a Global Development Research Scholarship to S.B. and H.C-Q in partnership with the USAID-Global Development Lab and the Peruvian and Brazilian USAID missions. S.B. also received support from the Lewis & Clark Fund for Exploration and Field Research in Astrobiology provided by the American Philosophical Society (APS). N.E.O. was funded in part by the DOE Great Lakes Bioenergy Research Center (DOE BER Office of Science DE-SC0018409).

Author contributions

S.B., N.E.O. and H.C.-Q. designed the study; S.B. conducted the field work with essential contributions from A.G.P-C, G.P.P., J.D.U.-M., L.P.R., J.F.-F., J.M.F.M., I.G.B. and B.G.; S.B., M.F.O., A.F.S., M.C.R., R.C. and J.P. performed laboratory experiments and molecular analyses; S.J.H. supported the NO analysis; K.E.H. conducted soil gamma sterilization; C.R.P. supported qPCR analysis. H.G. analysed isotopic abundances of gas samples; S.B., I.G.B., B.G., N.E.O. and H.C.-Q. performed the data analysis. S.B. and H.C.-Q. wrote the manuscript, and all co-authors contributed to the final version of the paper.

Competing interests

The authors declare no competing interests.

Additional information

Extended data is available for this paper at https://doi.org/10.1038/s41559-022-01892-y.

Supplementary information The online version contains supplementary material available at https://doi.org/10.1038/s41559-022-01892-y.

Correspondence and requests for materials should be addressed to Hinsby Cadillo-Quiroz.

Peer review information *Nature Ecology & Evolution* thanks Luiz Domeignoz, Maija Marushchak and Yit Arn Teh for their contribution to the peer review of this work. Peer reviewer reports are available.

https://doi.org/10.1038/s41559-022-01892-y

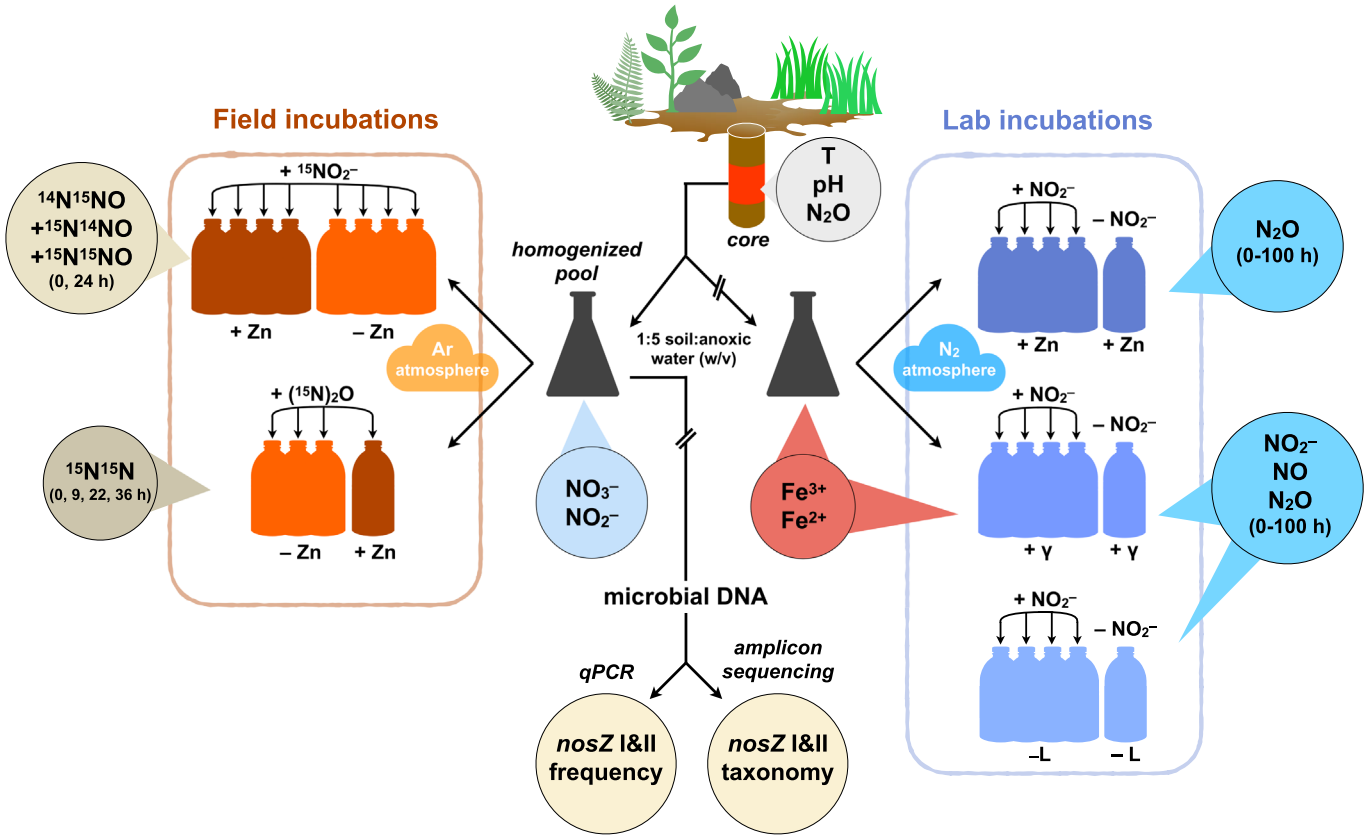

Extended Data Fig. 1 | Overall workflow of incubations in the field and lab. This workflow was applied for each peatland. Derived data sets are in circles. At the end of the incubations, microcosms were opened, and soil dry mass was determined for each replicate in order to normalize rates. Headspace of lab incubations was sporadically tested for CO_2 accumulation to verify absence of biological activity.

nature portfolio

Corresponding author(s): Hinsby Cadillo-Quiroz

Last updated by author(s): Aug 18, 2022

Reporting Summary

Nature Portfolio wishes to improve the reproducibility of the work that we publish. This form provides structure for consistency and transparency in reporting. For further information on Nature Portfolio policies, see our Editorial Policies and the Editorial Policy Checklist.

Statistics

For all statistical analyses, confirm that the following items are present in the figure legend, table legend, main text, or Methods section.

n/a	Confirmed
☐	☒ The exact sample size (*n*) for each experimental group/condition, given as a discrete number and unit of measurement
☐	☒ A statement on whether measurements were taken from distinct samples or whether the same sample was measured repeatedly
☐	☒ The statistical test(s) used AND whether they are one- or two-sided *Only common tests should be described solely by name; describe more complex techniques in the Methods section.*
☐	☒ A description of all covariates tested
☐	☒ A description of any assumptions or corrections, such as tests of normality and adjustment for multiple comparisons
☐	☒ A full description of the statistical parameters including central tendency (e.g. means) or other basic estimates (e.g. regression coefficient) AND variation (e.g. standard deviation) or associated estimates of uncertainty (e.g. confidence intervals)
☐	☒ For null hypothesis testing, the test statistic (e.g. *F*, *t*, *r*) with confidence intervals, effect sizes, degrees of freedom and *P* value noted *Give P values as exact values whenever suitable.*
☒	☐ For Bayesian analysis, information on the choice of priors and Markov chain Monte Carlo settings
☒	☐ For hierarchical and complex designs, identification of the appropriate level for tests and full reporting of outcomes
☒	☐ Estimates of effect sizes (e.g. Cohen's *d*, Pearson's *r*), indicating how they were calculated

Our web collection on statistics for biologists contains articles on many of the points above.

Software and code

Policy information about availability of computer code

Data collection	No software was used because empirical data was collected from experiments.
Data analysis	All statistical tests were performed with JMP Pro software (Version 13.1.0, SAS Institute Inc.). Analysis of variance (ANOVA) was used with $p < 0.05$ to test significantly different values for gene quantities across soils. Plotting and regression analysis were done with the Matlab R2018a software package (Version 9.4.0.813654, Mathworks Inc.).

For manuscripts utilizing custom algorithms or software that are central to the research but not yet described in published literature, software must be made available to editors and reviewers. We strongly encourage code deposition in a community repository (e.g. GitHub). See the Nature Portfolio guidelines for submitting code & software for further information.

Data

Policy information about availability of data

All manuscripts must include a data availability statement. This statement should provide the following information, where applicable:

- Accession codes, unique identifiers, or web links for publicly available datasets
- A description of any restrictions on data availability
- For clinical datasets or third party data, please ensure that the statement adheres to our policy

All data to evaluate the conclusions of the study are present in the paper, the Supplementary Information, and can be found in the Figshare repository (https://doi.org/10.6084/m9.figshare.19552588.v1). Genomic data have been deposited in the GenBank, EMBL, and DDBJ databases under accession: SAMN27959396,

SAMN27959397, SAMN27959398, SAMN27959399, SAMN27959400, SAMN27959401, SAMN27959402, SAMN27959403, SAMN27959404, SAMN27959405, SAMN27959406, SAMN27959407, SAMN27959408, SAMN27959409, SAMN27959410, SAMN27959411, SAMN27959412, SAMN27959413, SAMN27959414, SAMN27959415, SAMN27959416, SAMN27959417, SAMN27959418, SAMN27959419, SAMN27959420, SAMN27959421, SAMN27959422, SAMN27959423, SAMN27959424, SAMN27959425, SAMN27959426, SAMN27959427, SAMN27959428, SAMN27959429, SAMN27959430, SAMN27959431, SAMN27959432, SAMN27959433, SAMN27959434, SAMN27959435, SAMN27959436, SAMN27959437, SAMN27959438, SAMN27959439, SAMN27959440, SAMN27959441, SAMN27959442, and SAMN27959443

Human research participants

Policy information about studies involving human research participants and Sex and Gender in Research.

Reporting on sex and gender	NA
Population characteristics	NA
Recruitment	NA
Ethics oversight	NA

Note that full information on the approval of the study protocol must also be provided in the manuscript.

Field-specific reporting

Please select the one below that is the best fit for your research. If you are not sure, read the appropriate sections before making your selection.

☐ Life sciences ☐ Behavioural & social sciences ☒ Ecological, evolutionary & environmental sciences

For a reference copy of the document with all sections, see nature.com/documents/nr-reporting-summary-flat.pdf

Ecological, evolutionary & environmental sciences study design

All studies must disclose on these points even when the disclosure is negative.

Study description	Six peatlands were chosen to cover a geochemical spectrum, including acidic (pH 3.7-5) soils, low (10 µM) and high (> 5 mM) Fe2+ concentrations, varying OM content and soil temperature (Supplementary Table 4). Most sites were under little to no anthropogenic influence (Supplementary Table 5), with two exceptions: Fazenda Córrego da Areia (FCA) located within a catchment experiencing agricultural run-off in Brazil, and Medio Queso (MQE) in a Costa Rican river delta surrounded by agricultural run-off and cattle raising. The San Jorge (SJO) peatland is located in the Pastaza-Marañón foreland basin and Melendez (MEL) is in the Madre de Dios river terraces, both in Peru. Sítio do Cacau (SCB) is located in Central Amazonia (Amanã Reserve) in Brazil. Las Vueltas (VUL), located in Costa Rica's cloud forests of the Cerro Las Vueltas Reserve, differed most drastically from the other sites due to its higher altitude (2,500 m a.s.l.). Field work was conducted in September 2017 (Peru) and between April (Costa Rica) and July (Brazil) in 2018.
Research sample	The research samples were peat soils of selected peatlands (anoxic horizon, 2.5-7.5 cm depth) and headspace gas samples from incubations thereof.
Sampling strategy	Sampling was conducted based on biological triplicates and quadruplets. Previous testing showed technical replicates were consistent without significant variation.
Data collection	Data was collected by in-situ measurements and collected in a field notebook. Gas samples were collected by analyzer (GC and IRMS) and stored as text or excel files. Sequence data was collected at the to the DNASU core facility at Arizona State University.
Timing and spatial scale	Soil samples were sampled as soil cores spread over 1 square meter area. Gas samples from soil incubations were taken for (15N)2O analysis at the beginning of incubation and after 24 h (n = 4), and for 30N2 analysis at four time points spread over 36 h (n = 3) according to previous work (Babbins et al. 2015, Science).
Data exclusions	data points missing in specific analyses are listed in each figure or method section. Missing data was primarily originated by technical challenges including lack of gene amplification. No data exclusion was used.
Reproducibility	Experimental components when possible were repeated. In-situ incubations were not possible to repeat.
Randomization	Sample collection and evaluation when possible was completed in 50 m transects. Experimental set up of collected soil was tested with replicates where every sampled received the same treatment or control, which particular soil subsample received which treatment was done randomly.
Blinding	Blinding was not used as values of measurements are identified either at a later point than monitoring time or field samples were processed with codes not revealing structure of sampling although overall site belonging.

Did the study involve field work? ☒ Yes ☐ No

Field work, collection and transport

Field conditions	Six peatlands were chosen to cover a geochemical spectrum, including acidic (pH 3.7-5) soils, low (10 µM) and high (> 5 mM) Fe2+ concentrations, varying OM content and soil temperature (Supplementary Table 4). Most sites were under little to no anthropogenic influence (Supplementary Table 5), with two exceptions: Fazenda Córrego da Areia (FCA) located within a catchment experiencing agricultural run-off in Brazil, and Medio Queso (MQE) in a Costa Rican river delta surrounded by agricultural run-off and cattle raising. The San Jorge (SJO) peatland is located in the Pastaza-Marañón foreland basin and Melendez (MEL) is in the Madre de Dios river terraces, both in Peru. Sítio do Cacau (SCB) is located in Central Amazonia (Amanã Reserve) in Brazil. Las Vueltas (VUL), located in Costa Rica's cloud forests of the Cerro Las Vueltas Reserve, differed most drastically from the other sites due to its higher altitude (2,500 m a.s.l.). Field work was conducted in September 2017 (Peru) and between April (Costa Rica) and July (Brazil) in 2018.
Location	Site Code Latitude (°) Longitude (°): San Jorge, Iquitos, Peru SJO -4.058 -73.189 Melendez, Puerto Maldonado, Peru MEL -12.467 -69.178 Sítio do Cacau, Tefé, Brazil SCB -2.626 -64.593 Fazenda Córrego da Areia, Prados, Brazil FCA -21.024 -44.086 Las Vueltas, Dota, Costa Rica VUL 9.624 -83.848 Medio Queso, Los Chiles, Costa Rica MQE 11.038 -84.687
Access & import/export	Sampling was completed following the regulations that applied to protected, public or private locations across different study sites and their corresponding countries. Prior permitting, whenever possible, a research plan and sampling goals were submitted for permit approval. Access and Import permitting was approved under permit 0074-2015-SERFOR-DGGSPFFS and 0390-2016-SERFOR-DGGSPFFS plus private property approval for access in Peru, permit SINAC-ACAHN-PI-014-2018 in Costa Rica, and permit 033-2018-DEMUC-SEMAC and plus private property access approval in Brazil.
Disturbance	Disturbance was kept at a minimum. No material was left behind and no chemical waste was produced in the field.

Reporting for specific materials, systems and methods

We require information from authors about some types of materials, experimental systems and methods used in many studies. Here, indicate whether each material, system or method listed is relevant to your study. If you are not sure if a list item applies to your research, read the appropriate section before selecting a response.

Materials & experimental systems

n/a	Involved in the study
☒	☐ Antibodies
☒	☐ Eukaryotic cell lines
☒	☐ Palaeontology and archaeology
☒	☐ Animals and other organisms
☒	☐ Clinical data
☒	☐ Dual use research of concern

Methods

n/a	Involved in the study
☒	☐ ChIP-seq
☒	☐ Flow cytometry
☒	☐ MRI-based neuroimaging